

N⁷- and N⁹-substituted purine derivatives: a ¹⁵N NMR study

Radek Marek,^{1*} Jiří Brus,² Jaromír Toušek,³ Lajos Kovács⁴ and Dana Hocková⁵

¹ National Center for Biomolecular Research, Faculty of Science, Masaryk University, Kotlářská 2, CZ-61137 Brno, Czech Republic

² Institute of Macromolecular Chemistry, Academy of Sciences of the Czech Republic, Heyrovského náměstí 2, CZ-16206 Prague, Czech Republic

³ Department of Theoretical and Physical Chemistry, Faculty of Science, Masaryk University, Kotlářská 2, CZ-61137 Brno, Czech Republic

⁴ Department of Medicinal Chemistry, University of Szeged, Dóm tér 8, H-6720 Szeged, Hungary

⁵ Institute of Organic Chemistry and Biochemistry, Academy of Sciences of the Czech Republic, Flemingovo náměstí 2, CZ-16610 Prague, Czech Republic

Received 7 November 2001; Revised 10 January 2002; Accepted 13 January 2002

The ¹⁵N NMR chemical shifts of N⁷- and N⁹-substituted purine derivatives were investigated systematically at the natural abundance level of the ¹⁵N isotope. The NMR chemical shifts were determined and assigned using GSQMBBC, GHMBC, GHMQC and GHSQC experiments in solution. ¹⁵N cross-polarization magic angle spinning data were recorded for selected compounds in order to study the principal values of the ¹⁵N chemical shifts. Geometric parameters obtained by using RHF/6–31G** and single-crystal x-ray structural analysis were used to calculate the chemical-shielding constants (GIAO and IGLO) which were then used to assign the nitrogen resonances observed in the solid-state NMR spectra and to determine the orientation of the principal components of the shift tensors. Copyright © 2002 John Wiley & Sons, Ltd.

KEYWORDS: NMR; ¹H NMR; ¹⁵N NMR; isotropic chemical shifts; shift tensor; regio-isomerism; purine; quantum-chemical calculation

INTRODUCTION

N⁹-substituted analogs of natural purine nucleosides have been extensively investigated for their biological activity, especially as anticancer and antiviral compounds.^{1–3} N⁷-nucleoside analogs have been studied less frequently,^{4–7} often in context with N⁷/N⁹-glycosyl transfer.⁸ The standard method of choice for preparing N⁹-alkyladenines is the alkylation of the nucleobase in the presence of a base. The regioselectivity of this alkylation depends on the reaction conditions and on the nature of the purine base (e.g. substitution, protective groups, aza and deaza analogs). In most cases, the N⁷-regioisomer^{9–12} or N³-regioisomer^{13,14} is obtained as a side product of the N⁹-alkylation reaction. Predicting the site of alkylation is very difficult when protected or modified adenine is used. For example, we recently found that the alkylation of N⁶-(N,N-dimethylamino)methyleneadenine with certain alkylating reagents leads selectively to the N⁷-substituted derivatives.¹⁵ Alkylation of 2-aza- and 8-azaadenine produced the N²- and N⁸-substituted side products, respectively.^{16,17} In addition to standard ¹H and ¹³C NMR techniques, ¹H–¹⁵N

NMR experiments proved to be very useful in determining the position of the alkylation in these nitrogen-rich compounds.^{15,18}

In comparison with adenine, guanine displays a strikingly different behavior in glycosylation and alkylation reactions. Under the usual conditions, the N⁹- and N⁷-regioisomers form in a 1:1 ratio.^{19–21} This fact and the notoriously low solubility of guanine in most solvents²² render the substitution of guanine an unattractive task. A great deal of effort has been devoted to circumventing the above-mentioned problems^{23–26} and an exhaustive review details the available synthetic methods.²⁷ The site of the glycosylation or alkylation of guanine can be ascertained most conveniently by using 2D-NMR (¹H, ¹³C) techniques. Simple empirical rules based on the differences in the chemical shift of some diagnostic ¹³C signals have recently been found.²¹ Nonetheless, a study of protons and carbons conveys only indirect information about the nitrogen backbone, which is certainly the most sensitive to the pattern of N⁹/N⁷-substitution.

An extensive ¹⁵N NMR study of selected N⁷/N⁹-substituted purine analogs by Remaud *et al.*¹⁸ indicated considerable differences in the electronic structures between the pairs of N⁷/N⁹ isomers. ¹⁵N cross-polarization magic angle spinning (CP/MAS) spectra of adenine and guanine, including the determination of the principal components of the shift tensors, have been reported.²⁸ A ¹⁵N NMR study of the tautomerism of ¹⁵N-labeled adenine derivatives has also been published recently.²⁹

*Correspondence to: R. Marek, National Center for Biomolecular Research, Faculty of Science, Masaryk University, Kotlářská 2, CZ-61137 Brno, Czech Republic. E-mail: rmarek@chemi.muni.cz
Contract/grant sponsor: Ministry of Education of the Czech Republic; Contract/grant number: LN00A016.
Contract/grant sponsor: Grant Agency of the Czech Republic; Contract/grant number: 203/98/P026.
Contract/grant sponsor: Hungarian National Scientific Research Fund (OTKA); Contract/grant number: T 22551.

This contribution aims to give a detailed description of the differences in the electron distribution and the chemical shielding of the nitrogen atoms of selected N⁷/N⁹-substituted adenine and guanine derivatives. The compounds were investigated by using ¹⁵N NMR spectroscopy of the solid state and of solutions (especially by using inverse-detected experiments; for recent reviews see Refs 30 and 31). Quantum-chemical calculations of the ¹⁵N NMR parameters were also carried out. The structures of the guanine and adenine derivatives investigated are shown in Scheme 1.

RESULTS AND DISCUSSION

¹⁵N NMR chemical shifts of compounds 1–8 observed in DMSO-*d*₆ solutions were determined and assigned using gradient-enhanced ¹H–¹⁵N single-bond and especially multiple-bond chemical shift correlation experiments (GHMQC,³² GHSQC,^{33,34} GHMBC,^{34,35} GSQMB³⁶). The chemical shifts, reported relative to liquid ammonia,³⁷ are summarized in Table 1.

Using pulsed-field gradients to select a coherence pathway enabled us to observe very weak ¹H–¹⁵N interactions across up to four bonds (see Fig. 1) in experiments optimized for long-range couplings of 4.2–3.5 Hz (120–140 ms delay).

The detection of four-bond interactions was essential for assigning the N-1 and N-3 resonances of adenine derivatives 6 and 7. The cardinal asset was that the observation of

Table 1. ¹⁵N NMR chemical shifts^a of purine derivatives in DMSO-*d*₆^b at 303 K

Compound	N-1	N-3	N-7	N-9	N-10	N-12	N-17
1	152.4	201.1	165.6	250.5	137.1	—	—
2	153.5	182.8	249.2	156.6	137.4	—	—
3	— ^c	180.0	173.7	161.4	139.2	—	—
4	238.8	242.4	144.2	246.2	141.6	121.3 ^d	—
5a	235.6	221.8	239.4	153.6	142.1	120.9 ^d	—
5b	235.5	221.9	239.1	154.5	142.2	120.9 ^d	—
5c	235.5	222.2	238.7	155.6	142.1	— ^c	—
6a ^e	248.3	256.4	141.1	248.7	202.1	107.2	253.1
6b ^e	249.1	256.5	138.9	249.8	202.1	106.6	—
7a ^e	252.2	234.3	246.6	146.2	211.2	105.2	253.2
7b ^e	252.8	234.6	247.4	145.2	211.4	105.0	—
8	236.7	224.8	240.9	152.7	81.6	—	—

^a Referenced to 1 M urea in DMSO-*d*₆ (77.0 ppm)³⁷ and liquid CH₃NO₂ (381.7 ppm),³⁷ and reported relative to liquid NH₃.

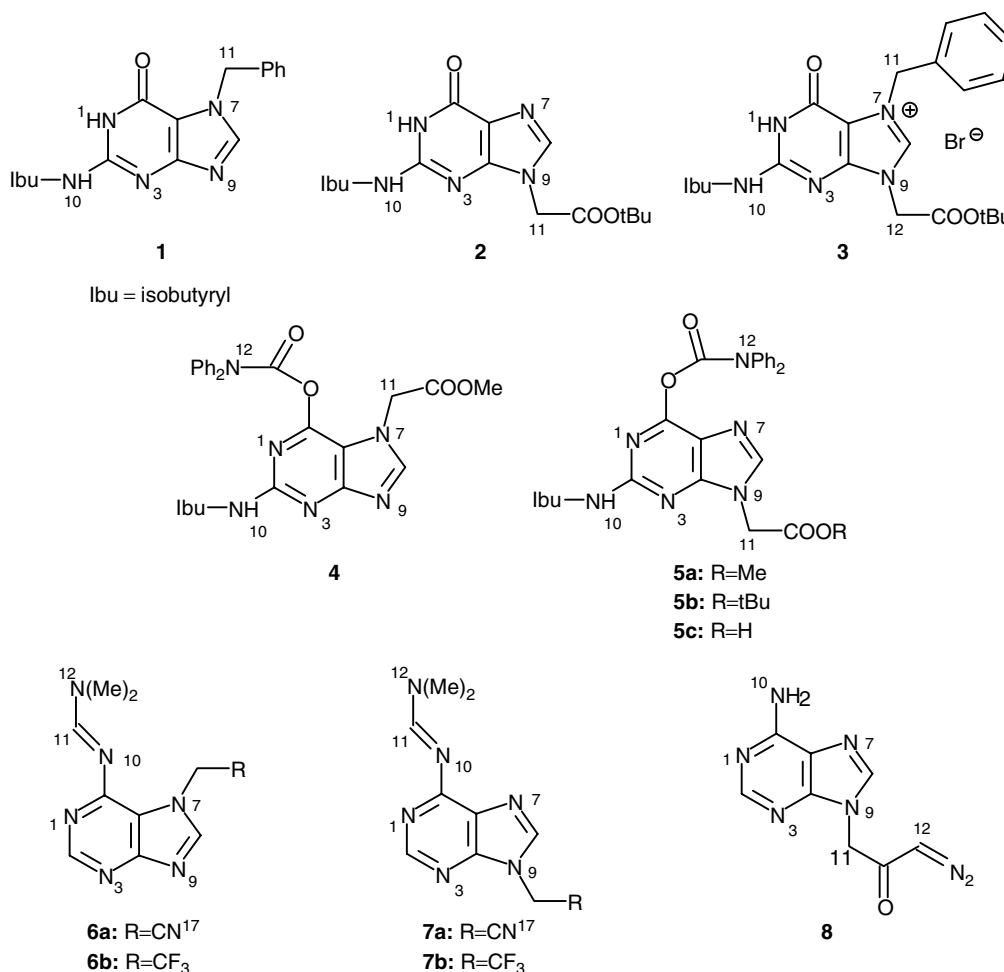
^b Commercially available deuterated solvent was used without further purification. The chemical shifts can be affected by water contained in the solvent.

^c Not observed.

^d Very weak response.

^e Ref. 15.

^f Adenine 235.8 (N-1), 230.1 (N-3), 80.2 (N-10).



Scheme 1

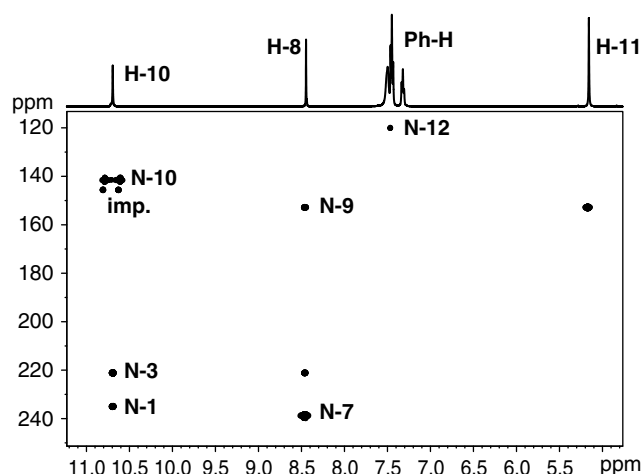


Figure 1. ¹H–¹⁵N GSQMBBC spectrum of 50 mg of compound **5a** at natural abundance dissolved in DMSO-*d*₆ (550 μl). The experiment was optimized for 4.2 Hz (120 ms delay) long-range coupling. The high-resolution proton spectrum is plotted atop the contour plot. Data acquisition parameters are specified in the Experimental section.

four-bond interactions allowed the chemical shifts of the N-3 atoms of the guanine derivatives (e.g. **3**) to be determined. The proton resonances of the H-10 atoms exhibit significant line broadening due to chemical-exchange processes (see Experimental). This chemical exchange precludes the detection of any interaction between H-10 and N-3 in long-range optimized chemical shift correlation experiments. Using the four-bond scalar interactions of N-3 and H-8 is the only way to determine the N-3 chemical shifts of such a structural arrangement (see Scheme 1) using inverse-detected experiments. The ¹H NMR chemical shifts, selected ¹H–¹⁵N long-range coupling constants, and corresponding signal half linewidths of selected guanine derivatives **1**–**5** are summarized in the Experimental section.

The solution-phase ¹⁵N NMR chemical shifts of the guanine 6-lactam and lactim (enolate) structures indicate that the N-1 and N-3 atoms of six-membered rings are significantly more shielded in the lactam derivatives **1** and **2**.³⁸ The change of nitrogen atom N-1 in compounds **4** and **5** compared with the lactam nitrogen in compounds **1** and **2** induces a resonance shift of ~80 ppm. The range of 150 ppm (N-1) for compounds **1** and **2** is characteristic of lactams thought of as being formed from the corresponding aromatic nitrogen heterocycles (e.g. oxoberberine³⁹). The nitrogen atom N-3 is 40 ppm more shielded in lactam derivatives **1** and **2**. The locking of the guanine moiety in the aromatic O⁶-acyl (lactim) derivatives (e.g. **4** and **5**) compared with the lactam structure (**1** and **2**) thus induces changes in the properties of the N-1 and N-3 nuclei approaching the properties of the NR₂-substituted adenine analogs (e.g. **8**).

The N-3 resonance shift of up to 73 ppm (for the guanine derivative **2** vs the adenine derivative **6**) is induced by the structural changes (see Table 1). Differences of up to 60 ppm are observed when the guanine lactam (**2**) and lactim (**4**) structures are compared. Extending the conjugation by transforming the —NH₂ group of the adenine into an —N=C moiety (compounds **6** and **7**) induces a downfield shift of

the resonances of the aromatic pyrimidine nitrogens N-1 and N-3. Derivatizing the free —NH₂ group (compound **8** and adenine) to form the imino —N=C moiety deshields the N-10 nitrogen atom by 120–130 ppm. The resonances of the N-10 atoms of guanine compounds **1**–**5** are found in the expected range of 137–143 ppm. Proton H-10 of the amide group resonates at ~11.6 ppm in compounds **1** and **2** whereas the H-10 resonance in compounds **4** and **5** is found at ~10.6 ppm. Proton–nitrogen coupling constants of ¹J(H,N) = 88–91 Hz were observed for the compounds investigated. The pyrrole-like nitrogen atoms of the five-membered ring resonate in the range 141–166 ppm whereas pyridine-like nitrogens exhibit chemical shifts of 238–251 ppm. The N-7 nitrogen atom is always more shielded than the N-9 atom in structurally related compounds. The directly detected ¹⁵N NMR spectra of regioisomers **4** and **5a** are shown in Fig. 2.

In order to study the individual components of the ¹⁵N shift tensors and their differences for pairs of N⁷/N⁹-isomers, ¹⁵N CP/MAS spectra were recorded and quantum-chemical calculations of the chemical shifts were carried out. The isotropic chemical shifts and the principal values of the chemical shifts were determined as the average values from two independent ¹⁵N CP/MAS experiments measured at different spinning frequencies. The values determined are summarized in Table 2.

The ¹⁵N resonances of a solid-state sample of the guanine derivative **5a** were easily assigned by comparing the data with the values obtained for a solution. The only exceptions were the assignments of the resonances of N-1 and N-7 at 229 and 236 ppm, respectively, which cannot be based on a straightforward comparison of the values for the solid state and the solution. The signal with a chemical shift of 236 ppm and a larger span of tensor components has been assigned to N-7 of the five-membered ring according to the quantum-chemical calculations (compare Table 4). The differences between the values obtained for the solid state and the solution are reasonably small (<3 ppm) for the indicated assignments with the exception of the N-1 resonance. This change of ~6.5 ppm could be attributed to differences in the intermolecular interactions involving the N-1 atom in the solid and the dissolved samples.

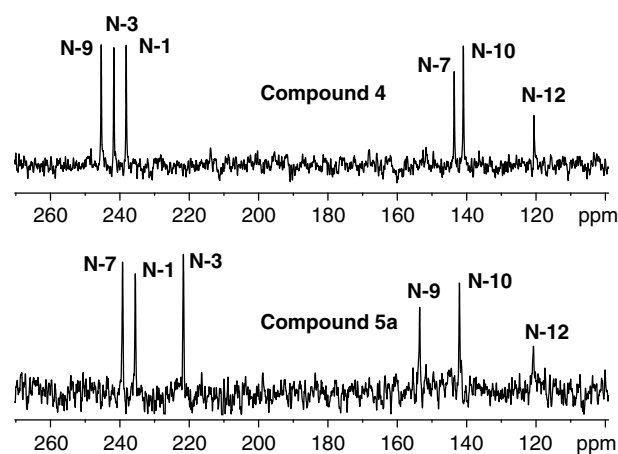


Figure 2. Directly detected ¹⁵N NMR spectra of regioisomers **4** and **5a** in DMSO-*d*₆ solutions.

Table 2. ^{15}N CP/MAS NMR data^a (relative to liquid NH_3) for derivatives **5a**, **6b** and **7a**

Compound	Parameter	N-1	N-3	N-7	N-9	N-10	N-12	N-17
5a	δ_{iso}	229.0	220.8	236.4	153.1	144.9	119.8	—
	δ_{11}^b	421.4	428.0	487.4	242.1	214.1	— ^f	—
	δ_{22}^b	190.5	215.7	211.3	146.4	132.6	— ^f	—
	δ_{33}^b	75.1	18.8	10.5	70.8	87.8	— ^f	—
	ξ^c	288.6	310.8	376.5	133.5	103.9	— ^f	—
	η^d	0.60	0.95	0.80	0.85	0.65	— ^f	—
	Span ^e	346.3	409.2	476.9	171.3	126.3	— ^f	—
6b	δ_{iso}	248.5	255.5	141.4	251.1	204.5	107.2	—
	δ_{11}^b	448.0	462.5	238.0	425.6	369.2	204.1	—
	δ_{22}^b	317.6	321.7	104.1	308.0	234.4	63.1	—
	δ_{33}^b	−19.9	−16.0	83.9	26.7	3.6	55.8	—
	ξ^c	299.2	309.7	144.0	258.2	250.2	144.6	—
	η^d	1.69	1.63	0.21	1.61	1.40	0.08	—
	Span ^e	467.9	478.5	154.1	398.9	365.6	148.3	—
7a	δ_{iso}	261.0	233.0	244.3	147.1	216.3	112.0	257.1
	δ_{11}^b	457.4	449.0	450.3	— ^f	401.4	— ^f	398.8
	δ_{22}^b	347.5	273.0	273.7	— ^f	215.4	— ^f	398.8
	δ_{33}^b	−13.1	−20.1	12.2	— ^f	36.4	— ^f	−23.6
	ξ^c	290.2	322.6	307.4	— ^f	275.5	— ^f	211.2
	η^d	1.84	1.36	1.27	— ^f	0.97	— ^f	2.98
	Span ^e	470.5	469.1	438.1	— ^f	365.0	— ^f	422.4

^a The isotropic chemical shifts and principal values of shift tensors (ppm) summarized in this table were determined as the average values from two independent ^{15}N CP/MAS NMR experiments measured at different spinning frequencies. The isotropic chemical shift was determined with an experimental error of ± 0.1 ppm; the experimental error in the determination of the principal values of the chemical shift oscillates in the range from ± 0.7 to ± 5.8 ppm.

^b δ_{11} , δ_{22} and δ_{33} (ppm) represent the three components of the shift tensor expressed in its principal axis system with the following rule: $\delta_{11} \geq \delta_{22} \geq \delta_{33}$.

^c Anisotropy parameter $\xi = (\delta_{11} - (\delta_{22} + \delta_{33})/2)$ (ppm).

^d Asymmetry parameter $\eta = |\delta_{22} - \delta_{33}|/|\delta_{11} - \delta_{\text{iso}}|$.

^e Span = $\delta_{11} - \delta_{33}$.

^f Value not determined.

Excellent agreement between the data for the solid state and the solution (<2.5 ppm; see Tables 1 and 2) allowed the assignment of the solid-state resonances of adenine derivative **6b** by a straightforward comparison of these data. The only resonances of the N-1 and N-9 atoms that are very close to each other ($\Delta\delta = 0.7$ ppm in the solution) were assigned by comparing their principal values and the span of the tensor components. Since the span of the tensor components of nitrogen atoms in five-membered rings is reduced due to the greater degree of localization of the six π -electrons⁴⁰ the signal at 251.1 ppm (span of components ~ 399 ppm) was assigned to the N-9 atom and the resonance at 248.5 ppm (span ~ 468 ppm) was assigned to the N-1 atom. The agreement between the calculated (see Table 4) and experimentally determined values of the respective δ_{33} components is likewise significant. The corresponding assignments are indicated in Table 2 and the ^{15}N CP/MAS spectrum of compound **6b** is shown in Fig. 3.

The differences between the data for the solid state and the solution were much larger for the N-9 substituted derivative **7a**. However, the separation of the resonance lines allowed relatively straightforward assignment of the individual signals. The proximal resonances of the N-1 and

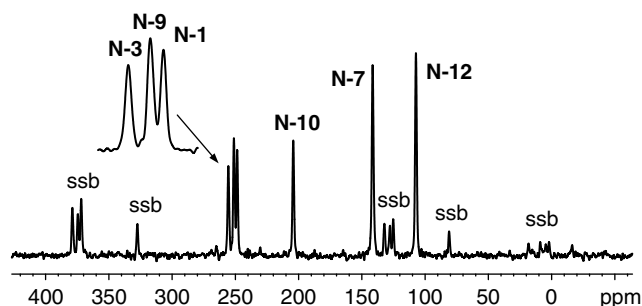


Figure 3. ^{15}N CP/MAS spectrum of compound **6b**. A magic angle spinning frequency 2.5 kHz was applied and 38 000 scans were accumulated.

the N-17 atoms were easily assigned based on the parameters of the axially symmetric shift tensor ($\delta_{11} = \delta_{22}$) of the CN group (see Table 2).

The geometries used as input files for the shielding calculations were obtained by either single-crystal x-ray structural analysis¹⁵ or quantum-chemical optimization of the geometry or both. The shielding information was obtained using GIAO⁴¹ and IGLO^{42,43} approaches. The

absolute values of the chemical shifts were calculated as the differences between the shielding constant of a standard (ammonia $\sigma_{\text{st}} = 245.07$)⁴⁴ and the shielding constant of each given molecule:

$$\delta_i = \sigma_{\text{st}} - \sigma_i$$

Since the relative agreement between the observed and calculated values is more important than the absolute shifts in assigning resonances, the computed values were shifted by the constant c (see Table 3). The constant c was found by minimizing the root mean square deviation (RMSD) between the observed and the calculated shift values for all ¹⁵N atoms.⁴⁵ The values of δ_{iso} of compound **6b** obtained by using several approaches are summarized in Table 3.

The best results were obtained when the geometry was optimized by using the RHF/6-31G** method and then the chemical shielding calculated by the B3LYP/6-31G** (see RMSD of **6b** in Table 3). This approach was applied to compounds **6** and **7**. Since the large numbers of atoms in **4** and **5a** required unacceptably long computational time (did not converge after several weeks), the geometries of **4** and **5a** were calculated by using the semiempirical AM1 method. All calculations were performed with an isolated molecule and no effects of the nearest neighbors were included.²⁸ Selected parameters of the ¹⁵N shift tensors are summarized in Table 4. The orientations of the individual components of the shielding tensors are in excellent agreement with the findings already published.⁴⁰

The nitrogen atom N-3 is significantly shielded, by ~20 ppm, in all the N⁹-isomers of both the adenine and guanine derivatives (compare values for **1** vs **2**, **4** vs **5** and **6** vs **7**).¹⁸ According to the solid-state NMR measurements and *ab initio* calculations, the change in the isotropic N-3 chemical shift is associated predominantly with the change in the δ_{22} component of the shift tensor (**6b** vs **7a**; see Table 2).

The orientation of this δ_{22} component was determined by quantum-chemical calculations to be approximately radial to the virtual direction of the free pair of electrons. Since the component in this direction is dominated by the orbitals lying in the plane perpendicular to its direction the change in shielding must be associated with changes in the $\sigma_{\text{N-C}}-\pi^*$ transitions (see Fig. 4).

On the other hand, *ab initio* calculations indicate that the change in the isotropic chemical shift of N-3 could also be associated with a change in the δ_{11} component (see Table 4). Clearly, an extensive study will be required in order to clarify the contribution of the δ_{11} component.

In conclusion, several facts should be highlighted. The experimental results show that the ¹⁵N chemical shifts in purines are very sensitive to structural changes. Even for the nitrogen atom N-3 at the same position of the purine skeleton the difference in the chemical shift in solution can be as much as 73 ppm (guanine derivative **2** vs adenine derivative **6**). Comparing the guanine lactam and lactim structures, differences of up to 60 ppm (**2** vs **4**) have been observed. The change in the chemical shielding of the N-3 nitrogen atom for an N⁷/N⁹ pair of regioisomers is associated predominantly with a change in the $\sigma_{\text{N-C}}-\pi^*$ transition that

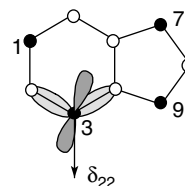


Figure 4. Schematic representation of the electron orbitals (the darker lobes are perpendicular to the plane of the molecule) making the largest contribution to the δ_{22} component of the shift tensor of the N-3 atom.

Table 3. *Ab initio* calculated values of ¹⁵N chemical shifts (ppm)^a for compounds **4**–**7**

Compound	N-1	N-3	N-7	N-9	N-10	N-12	N-17	RMSD	c
4 ^b	227.1	238.7	133.9	267.2	142.1	125.5	—	10.9	0.4
5a ^b	235.7	221.0	257.6	143.2	130.0	125.6	—	10.0	0.4
6a ^c	242.1	265.4	136.1	254.2	205.5	98.7	246.5	6.6	18.1
6b ^c	241.8	265.8	137.8	253.3	207.3	97.1	—	6.7	18.1
6b ^d	238.6	265.7	136.8	252.4	210.1	99.3	—	7.3	2.7
6b ^e	245.4	268.2	133.9	258.6	203.0	93.9	—	8.3	14.1
6b ^f	242.8	268.0	132.7	257.5	206.1	95.9	—	8.1	−0.7
7a ^c	241.3	227.2	253.5	144.4	213.1	102.5	256.4	6.2	18.1
7b ^c	240.9	229.0	250.7	146.0	213.6	101.2	—	5.9	18.1

^a The chemical shifts were calculated as the differences between the shielding constant of a standard (ammonia = 245.07)⁴⁴ and the shielding constants of a given molecule: $\delta_i = 245.07 - \sigma_i$. The chemical shifts were shifted by the constant c . The constant c was found by minimizing the root mean square deviation (RMSD) between the calculated values and the data observed in solution for all nitrogen atoms.⁴⁵ The same constant c was applied for all molecules calculated at the same level.

^b Geometry AM1; shielding B3LYP/6-31G**.

^c Geometry RHF/6-31G**; shielding B3LYP/6-31G**.

^d Geometry RHF/6-31G**; shielding IGLO II.

^e Geometry x-ray; shielding B3LYP/6-31G**.

^f Geometry x-ray; shielding IGLO II.

Table 4. *Ab initio* calculated^a values of the ¹⁵N chemical shifts (ppm) for compounds **5–7**

Compound	Parameter	N-1	N-3	N-7	N-9	N-10	N-12	N-17
5a^c	δ_{iso}	235.7	221.0	257.6	143.2	130.0	125.6	—
	δ_{11}	401.1	390.9	482.6	219.2	232.5	189.3	—
	δ_{22}	290.4	268.8	297.0	121.2	97.5	98.2	—
	δ_{33}	15.7	3.1	−6.9	79.3	60.1	89.3	—
	Span ^b	385.4	387.8	489.5	139.9	172.4	100.0	—
6a^d	δ_{iso}	242.1	265.4	136.1	254.2	205.5	98.7	246.5
	δ_{11}	434.8	484.7	221.5	449.6	365.8	188.6	403.5
	δ_{22}	326.3	343.0	118.9	307.5	251.2	76.2	396.9
	δ_{33}	−8.1	−4.4	95.1	32.6	26.3	58.5	−33.8
	Span ^b	442.9	489.1	126.4	417.0	339.5	130.1	437.3
6b^d	δ_{iso}	241.8	265.8	137.8	253.3	207.3	97.1	—
	δ_{11}	423.8	476.2	214.1	438.5	363.1	176.3	—
	δ_{22}	317.5	334.7	114.8	399.4	243.1	67.7	—
	δ_{33}	−16.0	−13.5	84.4	21.8	15.8	47.3	—
	Span ^b	439.8	489.7	129.7	416.7	347.3	129.0	—
7a^d	δ_{iso}	241.3	227.2	253.5	144.4	213.1	102.5	256.4
	δ_{11}	416.4	398.3	465.6	214.3	381.3	180.7	404.7
	δ_{22}	322.0	309.1	296.8	125.9	244.5	67.4	403.1
	δ_{33}	−14.4	−25.8	−2.0	92.9	13.4	59.4	−38.6
	Span ^b	430.8	424.1	467.6	121.4	367.9	121.3	443.3
7b^d	δ_{iso}	240.9	229.0	250.7	146.0	213.6	101.2	—
	δ_{11}	424.3	410.8	468.4	224.1	391.6	187.5	—
	δ_{22}	330.6	319.6	303.0	141.7	253.4	76.6	—
	δ_{33}	−5.3	−16.6	7.5	99.3	22.8	66.3	—
	Span ^b	429.6	427.4	460.9	124.8	368.8	121.2	—

^a The chemical shifts were calculated analogously to the procedure described in footnote a to Table 3 (geometry RHF/6–31G**; shielding B3LYP/6–31G**) with the exception of compound **5a** (geometry AM1; shielding B3LYP/6–31G**). The constant *c* was obtained as described in footnote a to Table 3.

^b Span = $\delta_{11} - \delta_{33}$.

^c *c* = 0.4.

^d *c* = 18.1.

dominates the δ_{22} component of the shift tensor. However, a better understanding of the factors determining these large changes in the chemical shifts must await the development of a comprehensive collection of ¹⁵N shift tensor data.

Our research on purine analogs is still in progress, and the effects of protonation and metal complexation on the NMR parameters of biologically related purines will be reported in forthcoming papers.

EXPERIMENTAL

Purine derivatives **1–8** were prepared according to the procedures described in the literature.^{15,21,46}

All solution-phase NMR spectra were recorded using a Bruker Avance DRX 500 spectrometer operating at frequencies of 500.13 MHz (¹H) and 50.68 MHz (¹⁵N). The temperature of the measurements was 303 K. Samples were prepared by dissolving 50 mg of the purine in 550 μ l of DMSO-*d*₆. The ¹⁵N resonances were referenced to the signal of 1 M urea in DMSO-*d*₆ (77.0 ppm) and liquid CH₃NO₂ (4 mm coaxial tube in a 5 mm tube with DMSO-*d*₆) (381.7 ppm).³⁷ The pulse conditions were 90° pulse,

duration 8.2–9.0 μ s for ¹H, 20.5 μ s for ¹⁵N (5 mm triple-resonance inverse probehead {¹H/BB/¹³C} equipped with a self-shielded z-gradient coil). Computer processing was performed with Bruker XWINNMR software.

GHSQC and GSQMBBC spectra were measured in the phase-sensitive mode (processed using the echo-antiecho protocol^{47–49}) and with magnetic field gradients. GHMQC and GHMBC spectra were processed in the magnitude mode. A gradient pulse duration of 1 ms and a post-gradient recovery delay of 100 μ s were used. The gradient ratios were 4.8:52.8:±4.8 G cm^{−1} for the ¹H–¹⁵N GHSQC and GSQMBBC experiments and 42:18:30 G cm^{−1} for the ¹H–¹⁵N GHMQC and GHMBC experiments. The delay for evolution of single- and multiple-bond couplings was set to 5.5 and 120–140 ms, respectively (with 2–32 transients accumulated per *t*₁ increment). Directly detected ¹⁵N NMR spectra were observed for samples prepared by dissolving 300 mg of the purine in 2.5 ml of DMSO-*d*₆ and using a BBO probehead (10 mm diameter) with a 15 μ s ¹⁵N pulse.

The ¹⁵N CP/MAS NMR spectra of solid samples were measured using a Bruker DSX 200 NMR spectrometer at a frequency of 20.28 and 200.14 MHz for ¹⁵N and ¹H,

respectively. Samples were placed in a 7 mm ZrO₂ rotor. The number of data points was 2K and the MAS frequency was 3–1 kHz. The strength of the *B*₁ field (for ¹⁵N and ¹H) for cross-polarization and the ¹H high-power decoupling were set to 32.9 and 62.5 kHz, respectively. The number of scans accumulated for the ¹⁵N CP/MAS NMR spectra was 22 000–64 000. A repetition delay of 4 s was used. The CP contact pulse was 1 ms. The ¹⁵N resonance was calibrated indirectly by using liquid CH₃NO₂ (δ = 381.7 ppm)³⁷ and solid NH₄Cl (δ = 40.7 ppm) externally. The parameters of the ¹⁵N shift tensor were calculated from the amplitudes of the spinning side bands by using the program package WIN-FIT (Bruker-Franzen Analytik). Owing to the relatively low signal-to-noise ratio (samples with the natural isotopic abundance of ¹⁵N were used) the values of the principal elements of the chemical shift tensor and the parameters of the CSA were determined with an experimental error of approximately ± 5 ppm. The isotropic chemical shifts were determined with an accuracy of ± 0.1 ppm.

Molecular geometries obtained by single-crystal x-ray analysis¹⁵ and/or *ab initio* optimization (RHF/6–31G**) were used for the quantum-chemical calculations. The shielding information was obtained by using the GIAO (B3LYP/6–31G**) method implemented in the Gaussian 94⁵⁰ and the IGLO (IGLO II) approach incorporated in the deMon/NMR⁵¹ code. All calculations were performed on SGI Power Challenge computers with R10000 processors in the supercomputing centers in Brno and Prague.

¹H NMR in DMSO-*d*₆ [atom number, half linewidth (Hz), ¹H, ¹⁵N coupling constant]: compound 1: 5.51 [H-11, 3.8], 8.33 [H-8, 2.9, ²*J*(H8,N7) = 7.3 Hz, ²*J*(H8,N9) = 11.6 Hz], 11.53 [H-10, 5.5], 12.14 [H-1, 6.9]; compound 2: 4.87 [H-11, 3.2], 7.94 [H-8, 2.3, ²*J*(H8,N7) = 12.2 Hz, ²*J*(H8,N9) = 8.1 Hz], 11.63 [H-10, 9.8], 12.09 [H-1, 9.7]; compound 3: 5.18 [H-12, 2.3], 5.81 [H-11, 2.7], 9.85 [H-8, 1.8], 12.10 [H-10, 9.1]*, 12.67 [H-1, 42.1]* (asterisks indicate values that may be exchanged); compound 4: 5.20 [H-11, 3.7], 8.55 [H-8, 2.4, ²*J*(H8,N7) = 7.1 Hz, ²*J*(H8,N9) = 12.3 Hz], 10.58 [H-10, 3.7]; compound 5a: 5.16 [H-11, 3.6], 8.44 [H-8, 2.3, ²*J*(H8,N7) = 12.8 Hz, ²*J*(H8,N9) = 8.6 Hz], 10.67 [H-10, 3.7]; compound 5c: 5.02 [H-11, 4.0], 8.44 [H-8, 2.6, ²*J*(H8,N7) = 12.5 Hz, ²*J*(H8,N9) = 7.8 Hz], 10.66 [H-10, 3.9]; compound 8: 5.06 [H-11, 10.4], 6.17 [H-12, 13.3], 7.28 [H-10, 6.3, ¹*J*(H10,N10) = 90 Hz], 8.08 [H-8, 3.0, ²*J*(H8,N7) = 12.1 Hz, ²*J*(H8,N9) = 8.3 Hz], 8.14 [H-2, 2.7].

Acknowledgments

This work was supported by grants from the Ministry of Education of the Czech Republic (LN00A016) (R.M.), the Grant Agency of the Czech Republic (203/98/P026) (D.H.) and the Hungarian National Scientific Research Fund (OTKA) (T 22551) (L.K.). We express our gratitude to the staff members of the supercomputing centers in Brno and Prague for CPU time.

REFERENCES

- Huryn DM, Okabe M. *Chem. Rev.* 1992; **92**: 1745.
- Holý A. In *Advances in Antiviral Drug Design*, vol. 1, De Clercq E (ed.). JAI Press: Greenwich, CT, 1993; 179–232.
- Holý A, Dvořáková H, Jindřich J. In *Antibiotics and Antiviral Compounds*, Krohn K, Kirst HA, Maag H (eds). VCH: Weinheim, 1993; 455–462.
- Seela F, Winter H. *Helv. Chim. Acta* 1994; **77**: 597.
- Rousseau RJ, Robins RK, Townsend LB. *J. Am. Chem. Soc.* 1968; **90**: 2661.
- Leonard NJ, Fujii T, Saito T. *Chem. Pharm. Bull.* 1986; **34**: 2037.
- Hocková D, Masojídková M, Holý A. *Collect. Czech. Chem. Commun.* 1999; **64**: 1316.
- Boryski J. *Nucleosides Nucleotides* 1996; **15**: 771.
- Raie S, Pongracic M, Vorkapic-Furac J, Vikić-Topić D, Hergold-Brundic A. *Nucleosides Nucleotides* 1996; **15**: 937.
- Hasan A, Srivastava PC. *J. Med. Chem.* 1992; **35**: 1435.
- Svansson L, Kvarström J. *J. Org. Chem.* 1991; **56**: 2993.
- Okumura K, Oine T, Yamada Y, Tomie M, Adachi T, Nagura T, Kawazu M, Mizoguchi T, Inoue I. *J. Org. Chem.* 1971; **36**: 1573.
- Janeba Z, Holý A, Masojídková M. *Collect. Czech. Chem. Commun.* 2000; **65**: 1126.
- Meszárosová K, Holý A, Masojídková M. *Collect. Czech. Chem. Commun.* 2000; **65**: 1109.
- Hocková D, Buděšínský M, Marek R, Marek J, Holý A. *Eur. J. Org. Chem.* 1999; 2675.
- Hocková D, Masojídková M, Buděšínský M, Holý A. *Collect. Czech. Chem. Commun.* 1995; **60**: 224.
- Holý A, Dvořáková H, Jindřich J, Masojídková M, Buděšínský M, Balzarini J, Andrei G, DeClercq E. *J. Med. Chem.* 1996; **39**: 4073.
- Remaud G, Kjellberg J, Bazin H, Johansson NG, Chattopadhyaya J. *Tetrahedron* 1986; **42**: 5073.
- Kjellberg J, Hagberg C-E, Malm A, Noren JO, Johansson N-G. *Acta Chem. Scand., Ser. B* 1986; **40**: 310.
- Kjellberg J, Johansson N-G. *J. Heterocycl. Chem.* 1986; **23**: 625.
- Timár Z, Kovács L, Kovács G, Schmel Z. *J. Chem. Soc., Perkin Trans.1* 2000; 19.
- Tanabe T, Yamauchi K, Kinoshita M. *Bull. Chem. Soc. Jpn.* 1979; **52**: 259.
- Jenny TF, Schneider KC, Benner SA. *Nucleosides Nucleotides* 1992; **11**: 1257.
- Robins MJ, Zou R, Guo Z, Wnuk SF. *J. Org. Chem.* 1996; **61**: 9207.
- Izawa K, Shiragami H. *Pure Appl. Chem.* 1998; **70**: 313.
- Brand B, Reese CB, Song Q, Visintin C. *Tetrahedron* 1999; **55**: 5239.
- Clausen FP, Juhl-Christensen J. *Org. Prep. Proced. Int.* 1993; **25**: 375.
- Hu JZ, Facelli JC, Alderman DW, Pugmire RJ, Grant DM. *J. Am. Chem. Soc.* 1998; **120**: 9863.
- Laxer A, Major DT, Gottlieb HE, Fischer B. *J. Org. Chem.* 2001; **66**: 5463.
- Marek R, Lyčka A. *Curr. Org. Chem.* 2002; **6**: 35.
- Martin GE, Hadden CE. *J. Nat. Prod.* 2000; **63**: 543.
- Müller L. *J. Am. Chem. Soc.* 1979; **101**: 4481.
- Bodenhausen G, Ruben DJ. *Chem. Phys. Lett.* 1980; **69**: 185.
- Willker W, Leibfritz D, Kerssebaum R, Bermel W. *Magn. Reson. Chem.* 1993; **31**: 287.
- Bax A, Summers MF. *J. Am. Chem. Soc.* 1986; **108**: 2093.
- Marek R, Králík L, Sklenář V. *Tetrahedron Lett.* 1997; **38**: 665.
- Wishart DS, Bigam CG, Yao J, Abildgaard F, Dyson HJ, Oldfield E, Markley JL, Sykes BD. *J. Biomol. NMR* 1995; **6**: 135.
- Witanowski M, Stefaniak L, Webb GA. *Annu. Rep. NMR Spectrosc.* 1993; **25**: 1.
- Marek R, Humpa O, Dostál J, Slavík J, Sklenář V. *Magn. Reson. Chem.* 1999; **37**: 195.
- Solum MS, Altmann KL, Strohmeier M, Berges DA, Zhang Y, Facelli JC, Pugmire RJ, Grant DM. *J. Am. Chem. Soc.* 1997; **119**: 9804.
- Ditchfield R. *Mol. Phys.* 1974; **27**: 789.
- Kutzelnigg W. *Isr. J. Chem.* 1980; **19**: 193.
- Kutzelnigg W, Fleischer U, Schindler M. In *NMR—Basic Principles and Progress*, vol. 23, Diehl P, Fluck E, Günther H, Kosfeld R, Seelig J (eds). Springer: Heidelberg, 1990; 165–262.
- Jameson CJ, de Dios AC. *J. Chem. Phys.* 1991; **95**: 1069.
- Marek R, Toušek J, Dostál J, Slavík J, Dommissie R, Sklenář V. *Magn. Reson. Chem.* 1999; **37**: 781.
- Kovács L. *Molecules* 2000; **5**: M130.

47. Davis AL, Keeler J, Laue ED, Moskau D. *J. Magn. Reson.* 1992; **98**: 207.
48. Tolman JR, Chung J, Prestegard J. *J. Magn. Reson.* 1992; **98**: 462.
49. Boyd J, Soffe N, John BK, Plant D, Hurd RE. *J. Magn. Reson.* 1992; **98**: 660.
50. Frisch MJ, Trucks GW, Schlegel HB, Gill PMW, Johnson BG, Robb MA, Cheeseman JR, Keith T, Petersson GA, Montgomery JA, Raghavachari K, Al-Laham MA, Zakrzewski VG, Ortiz JV, Foresman JB, Cioslowski J, Stefanov BB, Nanayakkara A, Challacombe M, Peng CY, Ayala PY, Chen W, Wong MW, Andres JL, Replogle ES, Gomperts R, Martin RL, Fox DJ, Binkley JS, Defrees DJ, Baker J, Stewart JP, Head-Gordon M, Gonzalez C, Pople JA. *Gaussian 94, Revision D.4*. Gaussian: Pittsburg, PA, 1995.
51. Malkin VG, Malkina OL, Salahub DR. *MASTER-CS Program*. University of Montreal: Montreal, 1994.